Accepted Manuscript

Title: A New Series of Pyridazinone Derivatives as Cholinesterases Inhibitors: Synthesis, *In Vitro* Activity and Molecular Modeling Studies

Authors: Azime Berna Özçelik, Zeynep Özdemir, Suat Sari, Semra Utku, Mehtap Uysal

Please cite this article as: Özçelik AB, Özdemir Z, Sari S, Utku S, Uysal M, A New Series of Pyridazinone Derivatives as Cholinesterases Inhibitors: Synthesis, *In Vitro* Activity and Molecular Modeling Studies, *Pharmacological Reports* (2019), https://doi.org/10.1016/j.pharep.2019.07.006

A New Series of Pyridazinone Derivatives as Cholinesterases Inhibitors: Synthesis, *In Vitro* Activity and Molecular Modeling Studies

Running title: Anticholinesterase, pyridazinone derivatives

Azime Berna Özçelik[1*], Zeynep Özdemir[2], Suat Sari[3], Semra Utku[4], Mehtap Uysal[1]

[1]*Gazi University, Faculty of Pharmacy, Department of Pharmaceutical Chemistry, Ankara, Turkey*
[2] *İnönü University, Faculty of Pharmacy, Department of Pharmaceutical Chemistry, Malatya, Turkey*
[3]*Hacettepe University, Faculty of Pharmacy, Department of Pharmaceutical Chemistry, Ankara, Turkey*
[4]*Mersin University, Faculty of Pharmacy, Department of Pharmaceutical Chemistry, Mersin, Turkey*

*Correspondence: Assoc. Prof. Azime Berna ÖZÇELİK, Gazi University, Faculty of Pharmacy, Department of Pharmaceutical Chemistry, 06100, Ankara, Turkey.

Phone: +90 312 202 32 22

Fax: +90 312 223 50 18

e-mail: brndemirci@yahoo.com

GRAPHİCAL ABSTRACT

A series of 3(2*H*)-pyridazinone derivatives were synthesis and evaluated their acetylcholinesterase (AChE) and buthyrylcholinesterase (BChE) inhibitory activity. Compound **VI₂ₐ** emerged as a dual inhibitor with 25.02% and 51.70% inhibition against AChE and BChE, respectively. Through molecular docking studies we tried to provide insights into the inhibition mechanism of our compounds against both enzymes at molecular level.
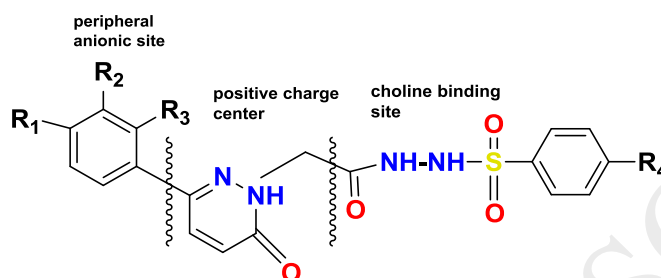
Research Highlights

- 12 new 3(2*H*)-pyridazinone derivative compounds have been synthesized.

- The anticholinesterase activity has been examined according to the Ellman Method.

- The structure-activity relationship of the synthesized compounds have been studied.

- Molecular docking studies have been performed.

Abstract

Background: The pyridazinone nucleus has been incorporated into a wide variety of therapeutically interesting molecules to transform them into better drugs. Acetylcholinesterase (AChE) and butyrylcholinesterase (BChE) are known to be serine hydrolase enzymes responsible for the hydrolysis of acetylcholine (ACh). Inhibition of cholinesterases is an effective method to curb Alzheimer's disease. Here, we prepared 12 new 6-substituted-3(*2H*)-pyridazinone-2-acetyl-2-(nonsubstituted/4-substituted benzenesulfonohydrazide) derivatives and evaluated their inhibitory effects on AChE/BChE in pursuit of potent dual inhibitors for Alzheirmer's Disease. We also tried to get insights into binding interactions of the synthesized compounds in the active site of both enzymes by using molecular docking approach.

Method: We obtained our compounds by the reaction of various substituted/nonsubstituted benzenesulfonic acid derivatives with 6-substitutedphenyl-3(*2H*)-pyridazinone-2-yl acetohydrazide and determined their anticholinesterase activities according to the Ellman's method. Molecular docking studies were done using Glide and the results were evaluated on Maestro (Schrödinger, LLC, New York, NY, 2019).

Results: The title compounds showed moderate inhibition at 100 µg/ml against both enzymes, yet with better activity against BChE. Compound **VI₂ₐ** emerged as a dual inhibitor with 25.02% and 51.70% inhibition against AChE and BChE, respectively.

Conclusion: This study supports that novel pyridazinone derivates may be used for the development of new BChE inhibitory agents. It was less potent than the reference drugs, yet promising for further modifications as a lead. The ability of the compounds to adopt energetically more favourable conformations and to engage in more key interactions in the ECBChE active gorge explains their better activity profile against ECBChE.

Introduction

Pyridazines are six-membered dinitrogen heterocycles often found in three different isomers, namely pyridazine (1,2-diazine), pyrimidine (1,3-diazine) and pyrazine (1,4-diazine) [1]. Nitrogen-containing heteroaromatic rings make up part of the bioactive compound space due to the coordination capability of nitrogen [2]. Recent studies have found that pyridazine is one of the most developable heteroaromatic rings for new drugs with eligibility to form ligands towards different targets, it is also found in the structure of natural compounds displaying various biological activities. Applications of substituted pyridazines as antidepressant, antihypertensive, anticonvulsant, antibacterial, diuretic, anti-HIV, anticancer, anti-inflammatory, analgesic, cardiovascular, and neuroprotective agents are available in the literature [3-13]. Some examples for medical use of pyridazine derivatives are zardaverine and imazodane as cardiotonic PDE III inhibitors and emorfazone as an analgesic agent (Figure 1) [6-8]. Xing et al. synthesized 2,6-disubstituted pyridazinone analogs and investigated their acetylcholinesterase (AChE) and butyrylcholinesterase (BChE) inhibitor activities. Among them, compound **4** was reported to be highly potent and selective against the cited enzymes (Figure 1) [14].

FIGURE 1

Figure 1. Structure of the drugs bearing pyridazinone skeleton and compound **4** [14].

Alzheimer disease (AD) is well-known for over a century, however, there is no concrete therapeutic treatment prevailed [15-17]. There is relationship between AD and changes in many neurotransmitters, including cholinergic, noncholinergic, serotonergic, dopaminergic, aminoacidergic, and neuropeptidergic; but the relationship between changes in the cholinergic system and AD is the most well-known. According to this relationship described as cholinergic hypothesis, decrease in acetylcholine and choline acetyl transferase levels is associated with AD [18]. Post-mortem brain studies and altered cholinergic symptoms such as degeneration of neurons controlling neocortical regions, loss of cholinergic terminals in the cerebral cortex, loss of choline acetyl transferase activity and acetyl choline synthesis, decreased cholinergic receptivity and increased AChE activity, which can be seen in many Alzheimer's patients [19,20]. For this reason, in the treatment of AD increasing acetylcholine level by suppressing AChE enzyme is one of the frequently used treatment modalities. On this basis, AChE inhibitors (AChEIs) have become the leading strategy for the development of anti-AD agents. The current

interest in these drugs has received considerable attention, too [21-23]. Some AChEIs, such as tacrine, donepezil, rivastigmine, and ensaculin (Figure 2), show modest improvement in memory and cognitive functions, and have been used to treat AD clinically for a long time. But only ensaculin, a coumarin derivative composed of benzopyran and a piperazine substituted moiety, has appeared to prevent or slow down the progressive neurodegeneration [22-25]. Ensaculin has been used clinically for the treatment of AD as an AChEI for a long time.

Although BChE is sparsely expressed in humans, recent studies proved that AChE inhibition alone may not be sufficient to reduce cholinesterase activity and choline levels may elevate since BChE makes up for the lost AChE activity. Furthermore, it is known that BChE expression is increased during AD [26,27]. Several studies, so far, have emphasized the importance of dual ChE inhibition in AD and other neurological disorders with cognitive decline. Drugs such as rivastigmin are efficacious in AD thanks to their dual-inhibitory character [28].

FIGURE 2

Figure 2. Structure of some FDA-approved AChEI in AD.

Zhou *et al*. designed and synthesized three different groups of coumarin-like compounds (A, B, C) bearing phenylpiperazine rings as substitution to evaluate their potential for treating AD (Figure 3) [25]. Zhou *et al.* also reported three hypothesis for the AChEI activity of their derivatives: (1) the coumarin ring, 2-(*H*)-chromen-2-one, a heterocyclic moiety involved in ensaculin's structure are responsible for cognitive functions and compatible with high anti-AChE potency, interacting with the peripheral anionic site (PAS); (2) the nitrogen atom from the phenylpiperazine group acting as the positive charge center presented in many potent AChE inhibitors, which can interact with the catalytic center of AChE demonstrated by the X-ray crystallographic studies of the AChE-donepezil and AChE-galantamine complexes, and (3) the phenyl ring is connected with the piperazine ring interacting with the cation-binding pocket (CBS) as shown in Figure 3 [25]. In addition, a linker chain bearing different numbers of carbon atom at the second position of the pyridazinone ringmight interact with the residues lining the wall of the AChE gorge.

FIGURE 3

Figure 3. Structural hypothesis for AChEIs and some designed compounds from the literature [25]

In view of the above mentioned findings, we designed and synthesized the title compounds (VI_{1a-1d}, VI_{2a-2d}, VI_{3a-3d}) to provide the structural requirements for AChEI and BChEI activities (Figure 4). We *in vitro* evaluated their AChE and BChE inhibitory effects using Ellman's method, the most commonly used method to measure cholinesterase activity [29].

FIGURE 4

Figure 4. Structural hypothesis for the title compounds [25].

The CBS moiety was designed as substituted phenyl ring and the structural modifications were focused on substitutions on the phenyl rings expected to interact with the CBS and PBS. Methoxy, chloro, bromo, and fluoro groups were included as substitutions on these rings at varying positions and combinations. Using molecular docking approach, we tried to predict binding interactions of our derivatives with AChE and BChE active sites and get insights into the structural attributes that affect their activities against these enzymes.

Materials and Methods

Chemistry

All chemicals used in this study were purchased from Aldrich, Fluka AG and E. Merck. 4-oxo-4-phenylbutanoic acid derivatives I_{1-3}, 6-substitutedphenyl-4,5-dihydropyridazin-3(2*H*)-one derivatives II_{1-3}, 6-substitutedphenylpyridazin-3(2*H*)-one derivatives III_{1-3}, 6-(substitutedphenyl) piperazine-1-yl)-3(2*H*)-on-2-yl acetate derivatives IV_{1-3} and 6-(substitutedphenyl)piperazine-1-yl)-3(2*H*)-on-2-yl acetohydrazide derivatives V_{1-3} were synthesized according to literature methods [30-33]. All title compounds VI_{1a-1d}, VI_{2a-2d}, VI_{3a-3d} were synthesized first time in this study according to the literature methods [34-36].

The purity of the compounds was checked by TLC with Merck Kieselgel F_{254} plates. Melting points were determined on Electrothermal 9200 melting points apparatus and the values were uncorrected. IR spectra were recorded on a Perkin Elmer Spectrometer by ATR technique. ^{1}H-NMR and ^{13}C-NMR spectra were recorded on a Brucker Avonce Ultrashield FT-NMR spectrometer in DMSO and $CDCl_3$ at 300 MHz in Inonu University, Malatya. The mass spectra (HRMS) of the compounds were recorded on Waters Acquity Ultra Performance Liquid Chromatograpy Micromass which combined LCT PremierTM XE UPLC/MS TOFF spectrophotometer (Waters Corp, Milford, USA) by ESI+ and ESI- techniques.

Synthesis of 4-oxo-4-phenylbutanoic acid derivatives (I_{1-3})

A mixture of 0.275 mol aluminum chloride, 20 ml carbon disulfide, and 0.25 mol succinicanhydride was added portion wise in standard conditions to a mixture of 0.25 mol 2-fluoroanisole and 50 ml carbon disulfide. Then the mixture was refluxed for 4 h at 40-50 °C. After cooling, the mixture was poured onto ice water and the precipitate was collected, dried and recrystallized from water [37].

Synthesis of 6-substitutedphenyl-4,5-dihydropyridazin-3(2H)-one derivatives (II$_{1-3}$)

0.01 Mol 4-(2-fluoro-4-methoxyphenyl)-4-oxobutanoic acid and 0.015 mol hydrazine hydrate (0.85 ml, 55%) in 30 ml ethanol were refluxed for 4 h. The reaction mixture was cooled and precipitate thus formed was collected by filtration, dried, and crystallized from ethanol [30].

Synthesis of 6-substitutedphenylpyridazin-3(2H)-one derivatives (III$_{1-3}$)

- **Method 1:**

A solution of 0.043 mol bromine in 25 ml glacial acetic acid was added drop wise to a solution of 0.039 mol 6-(2-fluoro-4-methoxyphenyl)-4,5-dihydro-3(2*H*)-pyridazinone in 100 ml glacial acetic acid at 60-70 °C, then the reaction mixture was refluxed for 3 h. After cooling to 5°C, it was poured into ice water and converted to the free base form with ammonium hydroxide. The precipitate was collected by filtration, washed with water until neutral, dried, and crystallized from ethanol-water [38].

- **Method 2:**

Glyoxylic acid (0.05 mol) and 4-chloro/bromo/methylacetophenone (0.15 mol) were heated at 100–105 °C for 2 h. At the end of this period, the reaction mixture was cooled to 40°C and 25% ammonium hydroxide solution was added to the reaction mixture until the pH of the medium reached 8. Then, the reaction mixture was extracted with dichloromethane (20 ml), the aqueous layer was separated and refluxed in the presence of hydrazine hydrate (0.05 mol) for 2 h. After the completion of the reaction, the mixture was cooled to room temperature. The resulting precipitate was filtered to give compounds **C1-3** [39-41].

Synthesis of ethyl 6-(substitutedphenyl)piperazine-1-yl)-3(2H)-on-2-yl acetate derivatives (IV$_{1-3}$)

A mixture of 0.01 mol proper 6-substituted phenylpyridazin-3(2*H*)-one derivative (***III$_{1-3}$***), 0.02 mol (2.2252 ml) ethyl bromoacetate, and 0.02 mol (2.7636 g) potassium carbonate in acetone (40 ml) was refluxed overnight. After the mixture was cooled, the organic salts were

filtered off, the solvent was evaporated, and the residue was purified by crystallization from methanol to give the esters [36].

Synthesis of 6-(substitutedphenyl)piperazine-1-yl)-3(2H)-on-2-yl acetohydrazide derivatives (V₁₋₃)

Hydrazine hydrate (99%, 3ml) was added to a solution of 0.01 mol proper ethyl 6-(substituted phenyl)piperazine-1-yl)-3(*2H*)-on-2-yl acetate derivative (*IV₁₋₃*) in 25 ml methanol and stirred for 3h at room temperature. The precipitate obtained was filtered off, washed with water, dried, and crystallized from ethanol [34].

General procedure for preparation of N'-[(substitutedphenyl)sulfonyl]-2-(6-(substitutedphenyl)-3(2H)-pyridazinone-2-yl)acetohydrazide (VI₁ₐ₋₁d, VI₂ₐ₋₂d, VI₃ₐ₋₃d)

Substituted benzenesulfonyl chloride (1 mmol) was added to a solution of proper 6-(substituted phenyl)piperazine-1-yl)-3(*2H*)-on-2-yl acetohydrazide derivative **(V₁₋₃)** (1 mmol) in pyridine (10 ml) at 0 °C. The resulting mixture was stirred at room temperature for 5 h. At the end of this period, the reaction mixture was poured into ice water. The precipitate was filtered, dried, and crystallized from an appropriate solvent. The compounds were identified by IR, ^{1}H-NMR, ^{13}C-NMR and mass spectra.

All spectral data of the compounds were in accordance with the assigned structures as shown below.

2-(3-(2-Fluoro-3-methoxyphenyl)-6-oxopyridazin-1(6H)-yl)-N'-(phenylsulfonyl)acetohydrazide (VI₁ₐ)

Yield: 59%; mp: 208ºC; ^{1}H-NMR (DMSO-*d₆*, 300 MHz): δ (ppm) 3.91 (3H; s; -OCH₃), 4.69 (2H; t; -N-CH₂-C=O), 7.05-8.09 (10H; m; phenyl protons and pyridazinone H^{4,5}), 10.02 (1H; s; -NH-C=O) and 10.42 (1H; s; -NH-SO₂). ^{13}C-NMR (DMSO-*d₆*, 300 MHz), δ 52.43 (1C; -OCH₃), 56.12 (1C; -N-C̲H₂-C=O), 112.99 (1C; phenyl C^2), 113.36 (1C; phenyl C^3), 113.95 (1C; phenyl C^4), 122.46 (1C; phenyl C^5), 126.97 (1C; phenyl C^6), 127.51 (1C; 2-fluoro-3-methoxyphenyl C^5), 128.81 (1C; 2-fluoro-3-methoxyhenyl C^6), 129.51 (1C; 2-fluoro-3-methoxyhenyl C^4), 130.87 (1C; pyridazinone C^5), 132.91 (1C; 2-fluoro-3-methoxyhenyl C^1), 138.93 (1C; pyridazinone C^6), 148.24 (1C; pyridazinone C^4), 149.96 (1C; 2-fluoro-3-methoxyphenyl C^2), 153.19 (1C; 2-fluoro-3-methoxyphenyl C^3), 158.65 (1C; phenyl C^1),

165.51 (1C; CH_2-N-$\underline{C}$=O), 170.67 (1C; pyridazinone C^3). $C_{19}H_{17}FN_4O_5S$. MS (ESI+) calculated: 433.0982, Found: *m/e* 433.0984 (M+H; % 100.0).

2-(3-(2-Fluoro-3-methoxyphenyl)-6-oxopyridazin-1(6H)-yl)-N'-(4-fluorophenylsulfonyl)acetohydrazide (VI$_{1b}$)

Yield: 94%; mp: 233°C; ^{1}H-NMR (DMSO-d_6, 300 MHz): δ (ppm) 3.90 (3H; s; -OCH$_3$), 4.70 (2H; t; -N-CH$_2$-C=O), 7.23-8.09 (9H; m; phenyl protons and pyridazinone H^{4,5}), 9.80 (1H; s; -NH-C=O) and 10.49 (1H; s; -NH-SO$_2$). ^{13}C-NMR (DMSO-d_6, 300 MHz), δ 52.55 (1C; -OCH$_3$), 56.08 (1C; -N-$\underline{C}$H$_2$-C=O), 112.95 (1C; 4-fluorophenyl C^2), 113.89 (1C; 4-fluorophenyl C^3), 115.81 (1C; 4-fluorophenyl C^6), 116.11 (1C; 4-fluorophenyl C^5), 122.41 (1C; 2-fluoro-3-methoxyphenyl C^5), 127.02 (1C; 2-fluoro-3-methoxyhenyl C^6), 129.47 (1C; 2-fluoro-3-methoxyhenyl C^4), 130.87 (1C; pyridazinone C^5), 135.12 (1C; 2-fluoro-3-methoxyhenyl C^1), 142.38 (1C; pyridazinone C^6), 148.09 (1C; pyridazinone C^4), 149.96 (1C; 4-fluorophenyl C^4), 153.19 (1C; 2-fluoro-3-methoxyphenyl C^2), 162.87 (1C; 2-fluoro-3-methoxyphenyl C^3), 165.56 (1C; 4-fluorophenyl C^1), 166.20 (1C; CH$_2$-N-$\underline{C}$=O), 170.66 (1C; pyridazinone C^3). $C_{19}H_{16}F_2N_4O_5S$. MS (ESI+) calculated: 451.0888, Found: *m/e* 451.0879 (M+H; % 100.0).

2-(3-(2-Fluoro-3-methoxyphenyl)-6-oxopyridazin-1(6H)-yl)-N'-(4-chlorophenylsulfonyl)acetohydrazide (VI$_{1c}$)

Yield: 89%; mp: 228°C; ^{1}H-NMR (DMSO-d_6, 300 MHz): δ (ppm) 3.90 (3H; s; -OCH3), 4.70 (2H; t; -N-CH2-C=O), 7.03-8.04 (9H; m; phenyl protons and pyridazinone H^{4,5}), 10.17 (1H; s; -NH-C=O) and 10.50 (1H; s; -NH-SO$_2$). ^{13}C-NMR (DMSO-d_6, 300 MHz), δ 52.56 (1C; -OCH$_3$), 56.12 (1C; -N-$\underline{C}$H$_2$-C=O), 112.99 (1C; 4-chlorophenyl C^2), 113.26 (1C; 4-chlorophenyl C^3), 113.96 (1C; 4-chlorophenyl C^6), 122.41 (1C; 4-chlorophenyl C^5), 123.87 (1C; 2-fluoro-3-methoxyphenyl C^5), 126.96 (1C; 2-fluoro-3-methoxyhenyl C^6), 129.51 (1C; 2-fluoro-3-methoxyhenyl C^4), 130.93 (1C; pyridazinone C^5), 136.09 (1C; 2-fluoro-3-methoxyhenyl C^1), 137.76 (1C; pyridazinone C^6), 142.41 (1C; pyridazinone C^4), 148.11 (1C; 4-chlorophenyl C^4), 149.58 (1C; 2-fluoro-3-methoxyphenyl C^2), 153.21 (1C; 2-fluoro-3-methoxyphenyl C^3), 158.65 (1C; 4-chlorophenyl C^1), 165.59 (1C; CH2-N-C=O), 170.62 (1C; pyridazinone C^3). $C_{19}H_{16}ClFN_4O_5S$. MS (ESI+) calculated: 467.0592, Found: *m/e* 467.0590 (M+H; % 100.0).

2-(3-(2-Fluoro-3-methoxyphenyl)-6-oxopyridazin-1(6H)-yl)-N'-(4-trifluoromethyl phenylsulfonyl)acetohydrazide (VI$_{1d}$)

Yield: 87%; mp: 240°C; ^{1}H-NMR (DMSO-d_6, 300 MHz): δ (ppm) 3.90 (3H; s; -OCH$_3$), 4.70 (2H; t; -N-CH$_2$-C=O), 7.01-8.10 (9H; m; phenyl protons and pyridazinone H^{4,5}), 10.35 (1H; s; -NH-C=O) and 10.56 (1H; s; -NH-SO$_2$). ^{13}C-NMR (DMSO-d_6, 300 MHz), δ 52.59 (1C; -OCH$_3$), 56.11 (1C; -N-$\underline{C}$H$_2$-C=O), 112.94 (1C; -CF$_3$), 113.20 (1C; 4-trifluoromethylphenyl C^2), 113.92 (1C; 4-trifluoromethylphenyl C^3), 122.41 (1C; 4-trifluoromethylphenyl C^6), 125.22 (1C; 4-trifluoromethylphenyl C^5), 125.98 (1C; 2-fluoro-3-methoxyphenyl C^5), 127.02 (1C; 2-fluoro-3-methoxyhenyl C^6), 128.55 (1C; 2-fluoro-3-methoxyhenyl C^4), 130.90 (1C; 4-trifluoromethylphenyl C^4), 132.28 (1C; pyridazinone C^5), 141.13 (1C; 2-fluoro-3-methoxyhenyl C^1), 142.88 (1C; pyridazinone C^6), 148.11 (1C; pyridazinone C^4), 148.25 (1C; 2-fluoro-3-methoxyphenyl C^2), 149.97 (1C; 2-fluoro-3-methoxyphenyl C^3), 153.21 (1C; 4-trifluoromethylphenyl C^1), 158.64 (1C; CH2-N-C=O), 165.71 (1C; pyridazinone C^3). C$_{20}$H$_{16}$F$_4$N$_4$O$_5$S. MS (ESI+) calculated: 501.0856, Found: *m/e* 501.0940 (M+H; % 100.0).

2-(3-(4-Chlorophenyl)-6-oxopyridazin-1(6H)-yl)-N'-(phenylsulfonyl)acetohydrazide (VI$_{2a}$)

Yield: 86%; mp: 198°C; ^{1}H-NMR (DMSO-d_6, 300 MHz): δ (ppm) 4.71 (2H; t; -N-CH$_2$-C=O), 7.10-8.10 (11H; m; phenyl protons and pyridazinone H^{4,5}), 10.03 (1H; s; -NH-C=O) and 10.44 (1H; s; -NH-SO$_2$). ^{13}C-NMR (DMSO-d_6, 300 MHz), δ 52.77 (1C; -N-$\underline{C}$H$_2$-C=O), 127.51 (1C; phenyl C^2), 127.56 (1C; phenyl C^3), 127.77 (1C; phenyl C^4), 128.83 (1C; phenyl C^5), 128.91 (1C; phenyl C^6), 129.42 (1C; 4-chlorophenyl C^2), 129.61 (1C; 4-chlorophenyl C^3), 131.02 (1C; pyridazinone C^5), 132.95 (1C; 4-chlorophenyl C^5), 133.62 (1C; 4-chlorophenyl C^6), 134.25 (1C; pyridazinone C^6), 137.30 (1C; pyridazinone C^4), 138.90 (1C; 4-chlorophenyl C^1), 142.52 (1C; 4-chlorophenyl C^4), 158.71 (1C; phenyl C^1), 165.45 (1C; CH$_2$-N-$\underline{C}$=O), 170.62 (1C; pyridazinone C^3). C$_{18}$H$_{15}$ClN$_4$O$_4$S. MS (ESI+) calculated: 419.0581, Found: *m/e* 419.0591 (M+H; % 100.0).

2-(3-(4-Chlorophenyl)-6-oxopyridazin-1(6H)-yl)-N'-(4-fluorophenylsulfonyl)acetohydrazide (VI$_{2b}$)

Yield: 79%; mp: 212°C; ^{1}H-NMR (DMSO-d_6, 300 MHz): δ (ppm) 4.71 (2H; t; -N-CH$_2$-C=O), 7.06-8.11 (10H; m; phenyl protons and pyridazinone H^{4,5}), 10.09 (1H; s; -NH-C=O) and 10.48 (1H; s; -NH-SO$_2$). ^{13}C-NMR (DMSO-d_6, 300 MHz), δ 52.59 (1C; -N-$\underline{C}$H$_2$-C=O), 115.84 (1C; 4-chlorophenyl C^2), 116.14 (1C; 4-chlorophenyl C^3), 116.79 (1C; 4-chlorophenyl C^5), 127.55 (1C; 4-chlorophenyl C^6), 128.91 (1C; 4-fluorophenyl C^2), 129.61 (1C; 4-fluorophenyl C^3), 130.63 (1C; pyridazinone C^5), 131.06 (1C; 4-fluorophenyl C^5), 132.95 (1C; 4-fluorophenyl C^6), 134.25 (1C; pyridazinone C^6), 135.14 (1C; pyridazinone C^4), 142.54 (1C; 4-chlorophenyl C^1),

158.71 (1C; 4-fluorophenyl C^1), 162.87 (1C; 4-chlorophenyl C^4), 165.47 (1C; 4-fluorophenyl C^4), 166.20 (1C; CH_2-N-$\underline{C}$=O), 170.58 (1C; pyridazinone C^3). $C_{18}H_{14}ClFN_4O_4S$. MS (ESI+) calculated: 437.0487, Found: *m/e* 437.0493 (M+H; % 100.0).

2-(3-(4-Chlorophenyl)-6-oxopyridazin-1(6H)-yl)-N'-(4-chlorophenylsulfonyl)acetohydrazide (VI₂c)

Yield: 86%; mp: 244°C; ^{1}H-NMR (DMSO-d_6, 300 MHz): δ (ppm) 4.71 (2H; t; -N-CH_2-C=O), 7.06-8.11 (10H; m; phenyl protons and pyridazinone $H^{4,5}$), 10.19 (1H; s; -NH-C=O) and 10.51 (1H; s; -NH-SO₂). ^{13}C-NMR (DMSO-d_6, 300 MHz), δ 52.61 (1C; -N-$\underline{C}H_2$-C=O), 127.56 (2C; 4-chlorophenyl^1 $C^{2,6}$), 128.93 (1C; 4-chlorophenyl^1 C^3), 129.52 (1C; 4-chlorophenyl^1 C^5), 129.81 (1C; pyridazinone C^5), 131.08 (2C; 4-chlorophenyl^2 $C^{3,5}$), 132.95 (2C; 4-chlorophenyl^2 $C^{2,6}$), 134.26 (1C; pyridazinone C^6), 136.07 (1C; pyridazinone C^4), 137.73 (1C; 4-chlorophenyl^1 C^1), 137.85 (1C; 4-chlorophenyl^2 C^1), 142.57 (1C; 4-chlorophenyl^1 C^4), 158.87 (1C; 4-chlorophenyl^2 C^4), 165.52 (1C; CH_2-N-$\underline{C}$=O), 170.56 (1C; pyridazinone C^3). $C_{18}H_{14}Cl_2N_4O_4S$. MS (ESI+) calculated: 453.0191, Found: *m/e* 453.0186 (M+H; % 100.0).

2-(3-(4-Chlorophenyl)-6-oxopyridazin-1(6H)-yl)-N'-(4-trifluoromethyl phenylsulfonyl)acetohydrazide (VI₂d)

Yield: 82%; mp: 229°C; ^{1}H-NMR (DMSO-d_6, 300 MHz): δ (ppm) 4.71 (2H; t; -N-CH_2-C=O), 7.05-8.12 (10H; m; phenyl protons and pyridazinone $H^{4,5}$), 10.34 (1H; s; -NH-C=O) and 10.55 (1H; s; -NH-SO₂). ^{13}C-NMR (DMSO-d_6, 300 MHz), δ 52.64 (1C; -N-$\underline{C}H_2$-C=O), 125.96 (1C; -CF₃), 126.01 (1C; 2-chlorophenyl C^1), 127.52 (2C; 4-trifluoromethylphenyl $C^{2,6}$), 128.56 (2C; 4-trifluoromethylphenyl $C^{3,5}$), 128.89 (4C; 2-chlorophenyl $C^{2,3,5,6}$), 129.58 (1C; 4-trifluoromethylphenyl C^1), 131.05 (1C; pyridazinone C^5), 132.92 (1C; 4-trifluoromethylphenyl C^4), 134.26(1C; pyridazinone C^6), 142.54(1C; pyridazinone C^4), 142.87 (1C; 4-chlorophenyl C^4), 158.70 (1C; CH_2-N-$\underline{C}$=O), 165.64 (1C; pyridazinone C^3). $C_{19}H_{14}ClF_3N_4O_4S$. MS (ESI+) calculated: 487.0455, Found: *m/e* 487.0462 (M+H; % 100.0).

2-(3-(4-Bromophenyl)-6-oxopyridazin-1(6H)-yl)-N'-(phenylsulfonyl)acetohydrazide   (VI₃a)

Yield: 78%; mp: 215°C; ^{1}H-NMR (DMSO-d_6, 300 MHz): δ (ppm) 4.76 (2H; t; -N-CH_2-C=O), 7.15-8.15 (11H; m; phenyl protons and pyridazinone $H^{4,5}$), 10.08 (1H; s; -NH-C=O) and 10.49 (1H; s; -NH-SO₂). ^{13}C-NMR (DMSO-d_6, 300 MHz), δ 52.56 (1C; -N-$\underline{C}H_2$-C=O), 122.94 (1C; phenyl C^4), 123.00 (1C; phenyl C^3), 127.51 (1C; 4-bromophenyl C^2), 127.81 (1C; 4-bromophenyl C^6), 128.83 (1C; phenyl C^5), 129,42 (1C; phenyl C^2), 129,62 (1C; phenyl C^6),

130.98 (1C; 4-bromophenyl C^3), 132.92 (1C; 4-bromophenyl C^5), 133.62 (1C; 4-bromophenyl C^4), 137.30 (1C; pyridazinone C^5), 138.90 (1C; pyridazinone C^6), 142.60 (1C; pyridazinone C^4), 158.71 (1C; phenyl C^1), 158.88 (1C; 4-bromophenyl C^4), 165.43 (1C; CH_2-N-$\underline{C}$=O), 170.61 (1C; pyridazinone C^3). $C_{18}H_{15}BrN_4O_4S$. MS (ESI+) calculated: 463.0076, Found: *m/e* 463.0102 (M+H; % 100.0).

2-(3-(4-Bromophenyl)-6-oxopyridazin-1(6H)-yl)-N'-(4-fluorophenylsulfonyl)acetohydrazide (VI$_{3b}$)

Yield: 87%; mp: 254°C; ^{1}H-NMR (DMSO-d_6, 300 MHz): δ (ppm) 4.76 (2H; t; -N-CH_2-C=O), 7.05-8.09 (10H; m; phenyl protons and pyridazinone $H^{4,5}$), 10.23 (1H; s; -NH-C=O) and 10.56 (1H; s; -NH-SO$_2$). ^{13}C-NMR (DMSO-d_6, 300 MHz), δ 52.62 (1C; -N-$\underline{C}H_2$-C=O), 123.00 (1C; 4-bromophenyl C^6), 127.81 (1C; 4-bromophenyl C^2), 128.97 (1C; 4-bromophenyl C^5), 129.51 (1C; 4-bromophenyl C^5), 129.61 (2C; 4-fluorophenyl $C^{3,5}$), 129.82 (2C; 4-fluorophenyl $C^{2,6}$), 131.04 (1C; pyridazinone C^5), 131.85 (1C; 4-bromophenyl C^1), 133.32 (1C; pyridazinone C^6), 137.74 (1C; pyridazinone C^4), 137.84 (1C; 4-fluorophenyl C^1), 142.65 (1C; 4-bromophenyl C^4), 158.72 (1C; 4-fluorophenyl C^4), 165.51 (1C; CH_2-N-$\underline{C}$=O), 170.56 (1C; pyridazinone C^3). $C_{18}H_{14}BrFN_4O_4S$ MS (ESI+) calculated: 481.2964, Found: *m/e* 480.9975 (M+H; % 100.0).

2-(3-(4-Bromophenyl)-6-oxopyridazin-1(6H)-yl)-N'-(4-chlorophenylsulfonyl)acetohydrazide (VI$_{3c}$)

Yield: 73%; mp: 225°C; ^{1}H-NMR (DMSO-d_6, 300 MHz): δ (ppm) 4.70 (2H; t; -N-CH_2-C=O), 7.06-8.11 (10H; m; phenyl protons and pyridazinone $H^{4,5}$), 10.09 (1H; s; -NH-C=O) and 10.48 (1H; s; -NH-SO$_2$). ^{13}C-NMR (DMSO-d_6, 300 MHz), δ 52.60 (1C; -N-$\underline{C}H_2$-C=O), 115.84 (2C; 4-bromophenyl $C^{2,6}$), 116.14 (1C; 4-bromophenyl C^5), 122.99 (1C; 4-bromophenyl C^5), 127.80 (2C; 4-chlorophenyl $C^{3,5}$), 129.61 (2C; 4-chlorophenyl $C^{2,6}$), 130.63 (1C; pyridazinone C^5), 130.76 (1C; 4-bromophenyl C^1), 131.02 (1C; pyridazinone C^6), 131.83 (1C; pyridazinone C^4), 133.31 (1C; 4-chlorophenyl C^1), 135.15 (1C; 4-bromophenyl C^4), 142.61 (1C; 4-chlorophenyl C^4), 158.71 (1C; CH_2-N-$\underline{C}$=O), 165.416 (1C; pyridazinone C^3). $C_{18}H_{14}BrClN_4O_4S$. MS (ESI+) calculated: 497.7480, Found: *m/e* 498.9678 (M+H; % 100.0).

2-(3-(4-Bromophenyl)-6-oxopyridazin-1(6H)-yl)-N'-(4-trifluoromethyl phenylsulfonyl)acetohydrazide (VI$_{3d}$)

Yield: 70%; mp: 255°C; ^{1}H-NMR (DMSO-d_6, 300 MHz): δ (ppm) 4.72 (2H; t; -N-CH_2-C=O), 7.04-8.11 (10H; m; phenyl protons and pyridazinone $H^{4,5}$), 10.35 (1H; s; -NH-C=O) and 10.56

(1H; s; -NH-SO$_2$). ^{13}C-NMR (DMSO-d_6, 300 MHz), δ 52.66 (1C; -N-$\underline{C}$H$_2$-C=O), 121.61 (1C; -CF$_3$), 123.001 (1C; 2-bromophenyl C^1), 125.23 (1C; 4-trifluoromethylphenyl C^2), 125.95 (1C; 4-trifluoromethylphenyl C^6), 126.00 (1C; 4-trifluoromethylphenyl C^3), 126.59 (1C; 4-trifluoromethylphenyl C^5), 127.75 (1C; 4-bromophenyl C^2), 127.82 (1C; 4-bromophenyl C^3), 128.55 (1C; 4-bromophenyl C^5), 129.58 (1C; 4-bromophenyl C^6), 130.99 (1C; 4-trifluoromethylphenyl C^1), 132.27 (1C; pyridazinone C^5), 133.36 (1C; 4-trifluoromethylphenyl C^4), 141.10 (1C; pyridazinone C^6), 142.87 (1C; pyridazinone C^4), 158.87 (1C; 4-bromophenyl C^4), 165.64 (1C; CH$_2$-N-$\underline{C}$=O), 170.62 (1C; pyridazinone C^3). C$_{19}$H$_{14}$BrF$_3$N$_4$O$_4$S. MS (ESI+) calculated: 531.3042, Found: m/e 530.9960 (M+H; % 100.0).

Pharmacology

Anticholinesterase Activity

The *in vitro* inhibition of AChE and BChE by the newly synthesized title compounds was determined by the method of Ellman et al. [29] using galantamine (CAS 357-70-0) as reference. Electric eel AChE (Type-VI-S, EC 3.1.1.7, Sigma, St. Louis, MO, USA) and horse serum BChE (EC 3.1.1.8, Sigma) as the enzyme sources, acetylthiocholine iodide and and butyrylthiocholine chloride (Sigma) as substrates, and 5,5'-dithio-bis(2-nitrobenzoic)acid (DTNB) were also used in the anticholinesterase activity determination. All reagents and conditions were the same as described recently [42]. Briefly, in this method, 140 μl 0.1 mM sodium phosphate buffer (pH8.0), 20 μl DTNB, 20 μl test solution, and 20 μl AChE/BChE solution were added by multichannel automatic pipette (Gilson pipetman, Middleton, USA) in a 96-well microplate and incubated for 15 min at 25°C. The reaction was then initiated with the addition of 10 μl acetylthiocholine iodide/butyryl-thiocholine chloride. The hydrolysis of acetylthiocholine iodide/butyrylthiocholine chloride was monitored by the formation of the yellow 5-thio-2-nitrobenzoate anion as a result of the reaction of DTNB with thiocholines catalyzed by the enzymes at a wavelength of 412 nm utilizing a 96-well microplate reader (VersaMax Molecular Devices, North Carolina, USA). The measurements and calculations were evaluated using Softmax PRO 4.3.2.LS software (Softmax Moleculer Devices, Downingtown, USA). The percentage of inhibition of AChE/BChE was determined by comparing the rates of the reactions of the samples relative to blank samples (ethanol in phosphate buffer pH= 8) using the formula (E-S)/E × 100, where E is the activity of the enzyme without test sample and S is the activity of the enzyme with the test sample. The experiments were done in triplicate and the results were expressed as average values with S.E.M. (standard error mean).

Molecular Modeling Methodology

Sequence alignment for EeAChE (O42275) and ECBChE (Q9N1N9) was performed using BLAST and Clustal Omega. The N terminal insertion residues of ECBChE were removed. The template structures, TcAChE (PDB ID: 6EUC [43]) and hBChE (PDB ID: 4TPK [44]), were downloaded from the RCSB protein data bank (www.rcsb.org) [45,46]. An initial 100 model structures were built by MODELLER (v9.19) for each enzyme using the sequence alignments and the template structures. The best model for each enzyme was selected according to the DOPE scores. Loop refinement was performed for the EeAChE model, which gave another 100 candidate models, again, the one with best DOPE score was selected. The final EeAChE and ECBChE models were submitted to PROCHECK server for analyses.

The model structures were prepared for docking using the Protein Preparation Wizard of Maestro (Schrödinger, LLC, New York, NY, 2019) [46]. In this process, the ionization and tautomeric states were generated by Epik (Schrödinger, LLC, New York, NY, 2019) and the proton orientations were set by PROPKA [47]. Restrained minimization was run using Impact (Schrödinger, LLC, New York, NY, 2019) with convergence of heavy atoms to an RMSD of 3 Å. The 3-D models of the ligands were created using MacroModel (Schrödinger, LLC, New York, NY, 2019), prepared for docking using LigPrep (Schrödinger, LLC, New York, NY, 2019) to include possible ionization and tautomeric states, and optimized using OPLS_2005 force field and conjugate gradient method [48]. The ligands were docked to the grids prepared by Grid generation module of Maestro using the central coordinates 56.74 164.35 183.69 for EeAChE and 4.33 10.44 14.00 for ECBChE. Docking procedure was performed 50 times for each ligand by Glide (Schrödinger, LLC, New York, NY, 2019) at extra precision with post-docking minimization enabled [49-51]. The docking score of each ligand was determined from the best pose upon visual evaluation on Maestro. RM0 and 3F9 were re-docked to their respective binding sites to test the performance of the docking methodology; the RMSD values of the resulting docking poses were 1.60 and 0.79, respectively.

Results

Chemistry

The title compounds (**VI$_{1a-1d}$**, **VI$_{2a-2d}$**, **VI$_{3a-3d}$**) were synthesized according to the literature methods as outlined in Scheme 1.

SCHEME 1

Scheme 1. Synthesis of the **VI$_{1a-1d}$**, **VI$_{2a-2d}$**, **VI$_{3a-3d}$**.

Synthesis of the compounds was initiated by obtaining benzoyl propanoic acid derivatives (**I₁₋₃**) in the presence of succinic anhydride and substituted benzene by anhydrous aluminum chloride catalysis. Subsequently, the reaction of these compounds with hydrazine hydrate led to the formation of 4,5-dihydro-3(*2H*)-pyridazinone (**II₁₋₃**) [52,53]. 6-Substituted-3(*2H*)-pyridazinone derivatives (**III₁₋₃**) were obtained by hydrolysis of **II₁₋₃** heated in glacial acetic acid [34]. A very useful and easy-to-use method was also tested for synthesis of compound **III₁₋₃**, which Schmidt and Druey developed in 1954 for the synthesis of pyridazinone compounds [54]. The reaction is based on the formation of 3(*2H*)-pyridazinone derivatives by condensation of 1,2-dicarbonyl compound with monosubstituted or unsubstituted hydrazine and the carboxyl derivative containing active methylene group. Dicarbonyl compounds including 1,2-diketones, α-ketoacids or glyoxal and esters, malonic acid, acetoacetic acid, cyanoacetic acid, benzoylacetic acid or hippuric acid esters are used as α-methylene reactive group [55]. In this study, glyoxalic acide was used as 1,2-dicarbonyl compound. Glyoxalic acid and acetophenone derivatives were heated with hydrazine hydrate in acidic medium to give 3(*2H*)-pyridazinone derivatives (**III₁₋₃**). Ethyl 6-substituted-3(*2H*)-pyridazinone-2-ylacetate derivatives (**IV₁₋₃**) were obtained by the reaction of **III₁₋₃** with ethyl bromoacetate in the presence of K_2CO_3 in acetone [34]. Then, 6-substituted-3(*2H*)-pyridazinone-2-ylacetohydrazide derivatives (**V₁₋₃**) were synthesized by the condensation reaction of **IV₁₋₃** with hydrazine hydrate [34]. Ultimately, the title compounds bearing benzenesulfonohydrazide structure were obtained by the reaction of **V₁₋₃** with substituted/nonsubstituted benzenesulfonylchlorides. All of the title compounds were reported for the first time in this study. The reaction yields ranged approximately from 60% to 90%. Compound **VI₁ᵦ** was synthesized with the highest yield (94%) while compound **VI₁ₐ** with the lowest yield (59%). The physical and spectral properties of the starting compounds were in accordance with the literature [35,56-60]. Molecular structures of title compounds were confirmed by IR, ^{1}H-NMR, ^{13}C-NMR, and mass spectral data. Their molecular structures, yields, and melting points are given in Table 1.

TABLE 1

Table 1. Molecular structures, yields and melting points of **VI₁ₐ₋₁ᵈ, VI₂ₐ₋₂ᵈ, VI₃ₐ₋₃ᵈ**

Pharmacology

*In vit*ro AChE and BChE inhibition of **VI$_{1a\text{-}1d}$**, **VI$_{2a\text{-}2d}$**, **VI$_{3a\text{-}3d}$** was determined by the method of Ellman et al. [29] using galantamine as reference. All compounds showed higher inhibitory activity against BChE than AChE. The activity data of the compounds were summarized as percentage inhibition ± standard deviation (SD) values at 50 and 100 µg/ml concentration in Table 2.

TABLE 2

Table 2. AChE and BChE inhibition percentages of the title compounds with ± standard error mean (SEM)

The compounds did not show AChE inhibition at 50 µg/ml. Compound **VI$_{1c}$** and **VI$_{2c}$** did not show AChE inhibition at 100 µg/ml, either. The inhibition % of **VI$_{3b}$** and **VI$_{3d}$** could not be measured because of precipitation at 100 µg/ml. The compounds were less potent than reference drugs, such as galantamine, donepezil, rivastigmine, physostigmine and tacrine but almost twice more potent against BChE than AChE. **VI$_{2a}$**, bearing 4-chlorophenyl ring, showed the best AChE inhibition with 25.02% and compound **VI$_{2a}$** showed the highest BChE inhibitory activity with a value of 51.70%. While compound **VI$_{2c}$** did not show AChE inhibitory activity, it was found to be the second most potent against BChE with a value of 51.36%. Compounds **VI$_{2c}$** and **VI$_{2d}$** showed high BChE inhibitor activity at low concentration compared to other compounds.

Molecular modelling studies

Homology modelling and structural evaluation of the enzyme structures

We built homology model of *Electrophorus electricus* (electric eel) AChE (EeAChE) and *Equus caballus* (horse) BChE (ECBChE) using comparative modelling techniques. The available crystal structures of EeAChE lack structural quality, resolution, and co-crystallized ligand to be useful in modelling studies and there is no crystal structure available for ECBChE. Homology modelling was performed by simply aligning the sequences of these enzymes with the most homologous sequences of the proteins with available 3D structure, *Tetronarce californica* AChE (TcAChE) and *Homo sapiens* BChE (hBChE), and threading the target model structures. (For the alignments, conserved and key residues see Figure S1 and S2 of Supporting Information). Sequence identitiy between EeAChE and TcAChE The co-crystallized inhibitors,

(*E*)-3-hydroxy-6-(5-morpholinopentyl)picolinaldehyde oxime (RM0) in TcAChE and *N*-{[(3*R*)-1-(2,3-dihydro-1*H*-inden-2-yl)piperidin-3-yl]methyl}-*N*-(2-methoxyethyl)naphthalene-2-carboxamide (3F9) in hBChE active gorge, as well as the solvent molecules, were transferred to the respective model structures using a specific MODELLER script [61]. A long insertion loop between residues 439-470 of EeAChE was optimized although these residues are away from the active gorge. In the case of ECBChE an insertion loop at the N terminal, which is far from the catalytic site, was removed. The PROCHECK analyses of the models confirmed their structural quality. The Ramachandran plot showed only 0.4% of the residues in the disallowed region for both models (See Figure S3 and S4 of Supporting Information), 99.6% of the planar groups of EeAChE and were within limits and this value was 100% for ECBChE. Regarding bad contacts, bond lengths, and angles both models were "1 1 2" in Morris et. al classification [62].

Molecular docking and binding interactions

The catalytic gorge of EeAChE accommodates several water molecules which take part in the water-mediated H bond network between RM0 and the receptor just like TcAChE, as well as π- π and π-cation interactions (Figure 5) [43]. In these interactions residues such as Tyr146, Ala226, Glu224, Trp304, Tyr355, Phe356, and His494 stood forward with direct or water-mediated contacts. The same interactions were observable with the corresponding residues in the template crystal structure. The counterparts of these residues in the *Homo sapiens* isozyme (HSAChE) reportedly play key role in accommodation of potent AChE ligands (see Table S1 in Supporting Information). For example, according to the literature studies, Tyr72 and Trp286, so-called PAS residues, stack with aromatic moieties of inhibitors close to the gorge entry. Asp74 (a PAS residue), Gly122, Glu202 (a choline binding pocket), Ala204, along with Tyr72 are known to participate in H bonds, some of which are water-mediated. Both Tyr337, a choline-binding pocket residue, and Phe338, which is an acyl-binding residue, are important for packing ligands in the cavity tightly. His447 is a member of the catalytic triad responsible for the esterase activity [60,63,64]. We observed in docking studies that galantamine also made water-mediated H bonds with Gu224 and His494 and π-π interaction with Tyr146 (Figure 5).

FIGURE 5

Figure 5. Binding interaction of RM0 (green), galantmine (gray), **1a** (teal) and **2a** (orange) (A-D, respectively) in EEChE active gorge. Ligands and water molecules are showed as color sticks, the active gorge residues in sticks and the protein backbone in tubes.

Our compounds bound the active gorge of EeAChE with high affinity (Table 3). Especially **1a** and **2a**, which were the most potent AChE inhibitors in the series, were among the derivatives with good scores. They bound to the EeAChE active site with the phenylpyridazinone moiety stretching to the bottom of the gorge and the phenylsulfonyl moiety occupying the PAS as demonstrated in Figure 5. Phenylpyridazinone moiety was mostly in hydrophobic contacts with the acyl- and choline-binding pocket residues of the CAS, defying the hypothesis of Zhou *et al.* [25]. Trp108, Trp304, and Tyr355 were among key residues in these interactions (see Figure S5 of Supporting Information for more details). Our compounds, however, failed in other key interactions listed above, especially H bonds and interactions with the catalytic triad, which could account for their limited potency against EeAChE compared to galantamine. Especially, lack of a positive charge group, a common pharmacophore among known AChE inhibitors, is one of the reasons for this situtation.

TABLE 3

Table 3. Docking scores

The complex of ECBChE and 3F9, a potent hBChE inhibitor [44], features several key interactions with the catalytic residues of the enzyme directly or mediated with water. Glu197 (choline-binding pocket), Trp231 and Phe329 (acyl-binding pocket), Asp70 and Tyr332 (PAS) are among the important residues to engage in these interactions (Figure 6). The exact same interactions with the exact same residues are observable between 3F9 and hBChE crystal structure as expected given the high level of homology between the two structures [44]. Docking pose of galantamine features interactions with Trp82 and Glu197 (choline-binding pocket) and His438 (catalytic triad) (Figure 6).

The title compounds fit in ECBChE active site with high affinity (Table 4). Their scores were as good as that of galantamin and potent derivatives ,for example, **2a** and **2c** were among the top scoring compounds. The compounds were observed to bind to the active gorge of ECBChE assuming a "V" shape taking a twist around the center of mass, unlike their straight binding orientations in EeAChE (Figure 6). The reason for this is the topology of the active gorge of BChE enzymes, which allows more conformational freedom in order to accommodate BCh, which has a bulkier acyl group than ACh [65]. In Figure 6 **2a** and **2c** are depicted docked to the enzyme and the key residues in their interactions include Trp82, Trp231, Leu285, and Phe329.

Along with conformational freedom, the title compounds engaged more in key interactions with ECBChE than with EeAChE (see Figure S6 of Supporting Information for more details), which probably made them more potent against the former and resulted in better docking scores (Table 4). Most of these residues were showed to be important for competitive inhibition through experimental and theoretical studies [44,60,66,67]. The binding mode of the title compounds in ECBChE active site were in accordance with the hypothesis presented by Zhou *et al.* [25] as summarized in Figure 4, which was not the case with EeAChE.

FIGURE 6

Figure 6. Binding interaction of 3F9 (green), galantmine (gray), **2a** (orange) and **2c** (magenta) (A-D, respectively) in ECBhE active gorge. Ligands and water molecules are showed as color sticks, the active gorge residues in sticks and the protein backbone in tubes.

Discussion

As a continuation of our research interest in developing novel 3(*2H*)-pyridazinone derivatives having AChEI and BChEI activities and establishing new relationships between their structure and activity, we designed and synthesized a series of 6-substituted-3(*2H*)-pyridazinone-2-acetyl-2-(nonsubstituted/4-substituted benzenesulfonohydrazide) and evaluated their AChE and BChE inhibitory activities according to the Ellman's method. The title compounds showed moderate inhibition at 100 µg/ml and they were more active against BChE. Compound **VI$_{2a}$** emerged as a dual inhibitor with 51.70% and 25.02% inhibition against AChE and BChE, respectively. In general, halogen substitution on benzalhydrazone phenyl ring leads to an increase in AChE and BChE inhibition. Cl and CF$_3$ substitutions at the *para* position of the benzalhydrazone phenyl ring also improved the anti-BChE activity. Adversely, *m*-substitutions on the benzalhydrazone phenyl ring with strong electron-donating groups such as OCH$_3$ reduced the AChE and BChE inhibition. It was less potent than the reference drugs, yet promising for further modifications as a leader.

With homology modelling we obtained reliabale and validated structure models of EeAChEand ECBChE. Molecular docking studies were very insightful for the structural features of the title compounds to engage in key interactons, as well as their shortcomings for ideal fit. Although the compounds showed high affinity to the enzymes, the lack of a positive charge group, for example, was apparent in docking studies, which could be a key aspect for future optimization of these derivatives into better inhibitors. The ability of the compounds to

adopt energetically more favourable conformations and to engage in more key interactions in the ECBChE active gorge explains their better activity profile against ECBChE.

Conflict of interest

All authors declare no conflict of interest connected with this paper.

References

[1] Coad P, Coad RA, Clough S, Hyepock J, Salisbury R, Wilkins C. Nucleophilic Substitution at the Pyridazine Ring Carbons. I. Synthesis of Iodopyridazines. J Org Chem 1963;28(1):218–221.

[2] Lamberth C. Pyridazine Chemistry in Crop Protection. Pest Manag Sci 2013;69:1106–1114.

[3] Asif M, Singh A, Lakshmayya. Development of structurally diverse antitubercular molecules with pyridazine ring. Chron Young Sci 2013;4:1-8.

[4] Asif M. Various Chemical and Biological Activities of Pyridazinone Derivatives. Cent Eur J Exp Biol 2017;5(1):1-19.

[5] Asif M. A brief review on Triazin-pyridazinones: Synthesis and biological activities. Mong J Chem 2016;17(43):28-33.

[6] Sato M. Effects of emorfazone on the nociceptive response induced by bradykinin in rats and dogs. Arch Int Pharmacodyn Ther 1982;257(2):200-212.

[7] Kips JC, Joos GF, Peleman RA, Pauwels RA. The effect of zardaverine, an inhibitor of phosphodiesterase isoenzymes III and IV, on endotoxin- induced airway changes in rats. Clin Exp Allergy 1993;23(6):518-523.

[8] El Rayes SM, Ali IAI, Fathalla W. Convenient Synthesis of Some Novel Pyridazinone-Bearing Triazole Moieties. J Heterocycl Chem 2019;56:51-59.

[9] Singh J, Sharma D, Bansal R. Synthesis and Biological Evaluation of 2- substituted- 6-(morpholinyl/piperidinyl)pyridazin- 3(2*H*)- ones as Potent and Safer Anti- inflammatory and Analgesic Agents. J Heterocycl Chem 2017;54(5):2935-2945.

[10] Sotelo E, Fraiz N, Yáñez M, Terrades V, Laguna R, Canob E, et al. Pyridazines. Part XXIX: synthesis and platelet aggregation inhibition activity of 5-substituted-6-phenyl-3(2H)-pyridazinones. Novel aspects of their biological actions. Bioorg Med Chem 2002;10(9):2873-2882.

[11] Akhtar W, Shaquiquzzaman M, Akhter M, Verma G, Khan MF, Alam MM. The therapeutic journey of pyridazinone. Eur J Med Chem 2016;123:256-281.

[12] Dubey S, Bhosle PA. Pyridazinone: an important element of pharmacophore possessing broad spectrum of activity. Med Chem Res 2015;24:3579–3598.

[13] Akhtar W, Verma G, Khan MF, Shaquiquzzaman M, Rana A, Anwer T, et al. Synthesis of Hybrids of Dihydropyrimidine and Pyridazinone as potential Anti-Breast Cancer Agents. Mini Rev Med Chem 2018;18:369-379.

[14] Xing W, Fu Y, Shi Z, Lu D, Zhang H, Hu Y. Discovery of novel 2,6-disubstituted pyridazinone derivatives as acetylcholinesterase inhibitors. Eur J Med Chem 2013;63:95–103.

[15] Rashid U, Ansari FL. Challenges in Designing Therapeutic Agents for Treating Alzheimer's Disease-from Serendipity to Rationality. Elsevier BV 2014;40-141.

[16] Geldenhuys WJ, Darvesh AS. Pharmacotherapy of Alzheimer's disease: current and future trends. Expert Rev Neurother 2015;5(1):3-5.

[17] Brookmeyer R, Abdalla N, Kawas CH, Corrada MM. Forecasting the prevalence of preclinical and clinical Alzheimer's disease in the United States. Alzheimers Dement 2018;14(2):121-129.

[18] Hampel H, Mesulam MM, Cuello AC, Farlow MR, Giacobini E, Grossberg GT, et al. The cholinergic system in the pathophysiology and treatment of Alzheimer's disease. Brain 2018;41:1917–1933.

[19] Tampi RR, Tampi DJ, Ghori AK. Acetylcholinesterase inhibitors for delirium in older adults. Am J Alzheimer Dis 2016;31(4):305–310.

[20] Belluti F, Bartolini M, Bottegoni G, Bisi A, Cavalli A, Andrisano V, et al. Benzophenone-based derivatives: a novel series of potent and selective dual inhibitors of acetylcholinesterase and acetylcholinesterase-induced betaamyloid aggregation. Eur J Med Chem 2011;46:1682-1693.

[21] Nakagawa R, Ohnishi T, Kobayashi H, Yamaoka T, Yajima T, Tanimura A, et al. Long-term effect of galantamine on cognitive function in patients with Alzheimer's disease versus a simulated disease trajectory: an observational study in the clinical setting. Neuropsychiatr Dis Treat 2017;13:1115-1124.

[22] Liu W, Wang H, Li X, Xu Y, Zhang J, Wang W, et al. Design, synthesis and evaluation of vilazodone-tacrine hybrids as multitarget-directed ligands against depression with cognitive impairment. Bioorg Med Chem 2018;26(12):3117-3125.

[23] Hu Y, Zhang J, Chandrashankra O, Ip FCF, Ip NY. Design, synthesis and evaluation of novel heterodimers of donepezil and huperzine fragments as acetylcholinesterase inhibitors. Bioorg Med Chem 2013;21:676–683.

[24] Caplan B, Bogner J, Brenner L, Malec J, Östberg A, Virta J, et al. Brain Cholinergic Function and Response to Rivastigmine in Patients With Chronic Sequels of Traumatic Brain Injury: A PET Study. J Head Trauma Rehabil 2018;33(1):25-32(8).

[25] Zhou Y, Wang S, Zhang Y. Catalytic reaction mechanism of acetylcholinesterase determined by born-oppenheimer AB initio QM/MM molecular dynamics simulations. J Phys Chem B 2010;114:8817–8825.

[26] Mesulam MM, Guillozet A, Shaw P. Widely spread butyrylcholinesterase can hydrolyze acetylcholine in the normal and Alzheimer brain. Neurobiol Dis 2002;9:88-93.

[27] Liu W, Wang H, Li X, Xu Y, Zhang J, Wang W, et al. Design, synthesis and evaluation of vilazodone-tacrine hybrids as multitarget-directed ligands against depression with cognitive impairment. Bioorg Med Chem 2018;26(12):3117-3125.

[28] Kandiah N, Pai MC, Senanarong V, Looi I, Ampil E, Park KW, et al. Rivastigmine: the advantages of dual inhibition of acetylcholinesterase and butyrylcholinesterase and its role in subcortical vascular dementia and Parkinson's disease dementia. Clin Interv Aging 2017;12:697–707.

[29] Ellman GL, Courtney KD, Andres V, Featherstone RM. A new and rapid colorimetric determination of acetylcholinesterase activity. Biochem Pharm 1961;7:88-95.

[30] Curran WV, Ross A. 6-Phenyl-4,5-dihydro-3(2*H*)-pyridazinones. A series of hypotensive agents. J Med Chem 1974;17(3)273-81.

[31] Demirayak S, Karaburun AC, Beis R. Some pyrrole substituted aryl pyridazinone and phthalazinone derivatives and their antihypertensive activities. Eur J Med Chem 2004;39:1089-1095.

[32] Gökçe M, Şahin MF, Küpeli E, Yeşilada E. Synthesis and Evaluation of the Analgesic and Anti-inflammatory Activity of New 3(2*H*)-Pyridazinone Derivatives. Arzneimittelforschung 2004;54(7):396-401.

[33] Boukharsa Y, Lakhlili W, El harti J, Meddah B, Tiendrebeogo, Taoufik J. Synthesis, anti-inflammatory evaluation in vivo and docking studies of some new 5-(benzo[b]furan-2-ylmethyl)-6-methyl-pyridazin-3(2*H*)-one derivatives. J Mol Struct 2018;153:19-127.

[34] Şahin MF, Badıçoglu B, Gökçe M, Küpeli E, Yeşilada E. Synthesis and analgesic and antiinflammatory activity of methyl[6-substitue-3(2H)-pyridazinone-2-yl]acetate derivatives. Arch.Pharm Pharm Med 2004;33:445–452.

[35] Özdemir Z, Yılmaz H, Sarı S, Karakurt A, Şenol FS, Uysal M. Design, synthesis, and molecular modeling of new 3(2*H*)-pyridazinone derivatives as acetylcholinesterase/ butyrylcholinesterase inhibitors. Med Chem Res 2017;26:2293-2308.

[36] Utku S, Gökçe M, Orhan İ, Şahin MF. Synthesis of novel 6-substituted-3(2*H*)-pyridazinone-2-acetyl-2-(substituted/-nonsubstituted benzal)hydrazone derivatives and acetylcholinesterase and butyrylcholinesterase inhibitory activities in vitro. Arzneim Forsch 2011;61:1–7.

[37] Loev B, Greenwald RB, Goodman MM, Zirkle CL. Benzazepinones. Synthesis of the monoaza analog of diazepam, and the correct structure of the benzoylpropionanilide cyclization product. J Med Chem 1971;14(9):849–852.

[38] Dorsch D, Stieber F, Stiryakichadt O, Blaukat A. Pyridazinone derivatives as Met kinase inhibitors and their preparation and use in the treatment of cancer. Merck Patent G.m.b.H., Germany, 2008.

[39] Tiryaki D, Şüküroğlu M, Doğruer DS, Akkol E, Özgen S, Şahin MF. Synthesis of some new 2,6-disubstituted-3(2H)-pyridazinone derivatives and investigation of their analgesic, anti-inflammatory and antimicrobial activities. Med Chem Res 2013;22:2553–2560.

[40] Gökçe M, Utku S, Küpeli E. Synthesis and analgesic and anti-inflammatory activities 6-substituted-3(2H)-pyridazinone-2-acetyl-2-(p-substituted/nonsubstituted benzal)hydrazone derivatives. Eur J Med Chem 2009;44(9):3760-3764.

[41] Coates WJ, Mckillop A. One-Pot Preparation of 6-Substituted 3(2H)-Pyridazinones from Ketones. Synthesis 1993;3:334-342.

[42] Orhan I, Aslan S, Kartal M, Şener B, Başer KHC. Inhibitory effect of Turkish Rosmarinus officinalis L. on acetylcholinesterase and butyrylcholinesterase enzymes. Food Chem 2008;108:663–668.

[43] Zorbaz T, Braiki A, Katalinic M, Renou J, de la Mora E, Mercey G, et al. Reactivation potency and blood-brain barrier penetration of 3-hydroxy-2-pyridine aldoximes in organophosphate poisoning (unpublished PDB entry).

[44] Brus B, Kosak, S. Turk A, Coquelle PN, Kos J, Stojan mximum J.P. Colletier, S. Gobec, Discovery, biological evaluation, and crystal structure of a novel nanomolar selective butyrylcholinesterase inhibitor. J Med Chem 2014;57:8167-8179.

[45] Berman HM, Westbrook J, Feng Z, Gilliland G, Bhat TN, Weissig H, et al. The Protein Data Bank Nucleic Acids Research. 2000;28:235-242.

[46] Sastry GM, Adzhigirey M, Day T, Annabhimoju R, Sherman W. Protein and ligand preparation: Parameters, protocols, and influence on virtual screening enrichments. J Comput Aid Mol Des 2013;27(3):221-234.

[47] Greenwood JR, Calkins D, Sullivan AP, Shelley JC. Towards the comprehensive, rapid, and accurate prediction of the favorable tautomeric states of drug-like molecules in aqueous solution. J Comput Aided Mol Des 2010;24:591-604.

[48] Banks L, Beard HS, Cao Y, Cho AE, Damm W, Farid R, et al. Integrated modeling program, applied chemical theory (IMPACT). J Comput Chem 2005;26:1752–1780.

[49] Friesner RA, Banks JL, Murphy RB, Halgren TA, Klicic JJ, Mainz DT, et al. Glide: a new approach for rapid, accurate docking and scoring. 1. Method and Assessment of Docking Accuracy. J Med Chem 2004;47:1739–1749.

[50] Friesner RA, Murphy RB, Repasky MP, Frye LL, Greenwood JR, Halgren TA, et al. Extra Precision Glide: Docking and Scoring Incorporating a Model of Hydrophobic Enclosure for Protein-Ligand Complexes. J Med Chem 2006;49:6177–6196.

[51] Halgren TA, Murphy RB, Friesner RA, Beard HS, Frye LL, Pollard WT, et al. Glide: a new approach for rapid, accurate docking and scoring. 2. Enrichment factors in database screening. J Med Chem 2004;47:1750–1759.

[52] Budhlakoti P, Kumar Y, Verma A, Alok S. Synthesis, antibacterial activity and molecular properties prediction of some pyridazin-3-one derivatives. Int J Pharm Sci Res 2013;4(4):1524-1528.

[53] Zare L, Mahmoodi NO, Yahyazadeh A, Nikpassand M. Ultrasound-promoted regio and chemoselective synthesis of pyridazinones and phthalazinones catalyzed by ionic liquid [bmim]Br/AlCl3. Ultrason Sonochem 2012;19:740–744.

[54] Schmidt P, Druey J. Heilmittelchemische Studien in der heterocyclischen Reihe. 10. Mitteilung. Pyridazine VII. Zur neuen Pyridazin-Synthese. Methylpyridazine. Helv Chim Acta 1954;37(5):1467-1471.

[55] Katritzky AR, Boulton AJ. Advances in Heterocyclic Chemistry (vol. 9). New York, London: Academic Press., 1968.

[56] Lapinski L, Nowak MJ, Fulara J, Les´ A, Adamowicz L. Relation between structure and tautomerism in diazinones and diazinethlones. An experimental matrix isolation and theoretical ab initio study. J Phys Chem 1992;96:6250–6254.

[57] Katritzky AR, Lagowski JM. Prototropic Tautomerism of Heteroaromatic Compounds: II. Six-Membered Rings. Adv Heterocycl Chem 1963;1:339-437.

[58] Radic Z, Pickering NA, Vellom DC, Camp S, Taylor P. Three distinct domains in the cholinesterase molecule confer selectivity for acetyl- and butyrylcholinesterase inhibitors. Biochemistry 1993;32(45):12074-12084.

[59] Mallender WD, Szegletes T, Rosenberry TL. Acetylthiocholine Binds to Asp74 at the Peripheral Site of Human Acetylcholinesterase as the First Step in the Catalytic Pathway. Biochemistry 2000;39(26):7753-7763.

[60] Rosenberry TL, Brazzolotto X, Macdonald IR, Wandhammer M, Trovaslet-Leroy M, Darvesh S, et al. Comparison of the Binding of Reversible Inhibitors to Human Butyrylcholinesterase and Acetylcholinesterase: A Crystallographic, Kinetic and Calorimetric Study. Molecules 2017;22:2098.

[61] Eswar N, Webb B, Marti-Renom MA, Madhusudhan MS, Eramian D, Shen MY, et al. Comparative protein structure modeling using Modeller. Curr Protoc Bioinformatics 2016 Chapter 5: Unit-5.6. doi: 10.1002/0471250953.bi0506s15.

[62] Morris AL, MacArthur MW, Hutchinson EG, Thornton JM. Stereochemical quality of protein structure coordinates. Proteins 1992;12(4):345-64.

[63] Cheung J, Rudolph JM, Burshteyn F, Cassidy MS, Gary EN, Love J, et al. Structures of Human Acetylcholinesterase in Complex with Pharmacologically Important Ligands. J Med Chem 2012;55:10282−10286.

[64] Bester SM, Guelta MA, Cheung J, Winemiller MD, Bae SY, Myslinski J, et al. Structural Insights of Stereospecific Inhibition of Human Acetylcholinesterase by VX and Subsequent Reactivation by HI‑ 6. Chem Res Toxicol 2018;31:1405-1417.

[65] Campiani G, Fattorusso C, Butini S, Gaeta A, Agnusdei M, Gemma S, et al. Development of molecular probes for the identification of extra interaction sites in the mid-gorge and peripheral sites of butyrylcholinesterase (BuChE). Rational design of novel, selective, and highly potent BuChE inhibitors. J Med Chem 2005;48(6):1919-29.

[66] Masson P, Froment MT, Bartels CF, Lockridge O. Asp70 in the peripheral anionic site of human butyrylcholinesterase. Eur J Biochem 1996;235:36-48.

[67] Macdonald IR, Martin E, Rosenberry TL, Darvesh S. Probing the peripheral site of human butyrylcholinesterase. Biochemistry 2012;51:7046–7053.

Figure captions:

Figure 1. Structure of the drugs bearing pyridazinone skeleton and compound **4** [14].
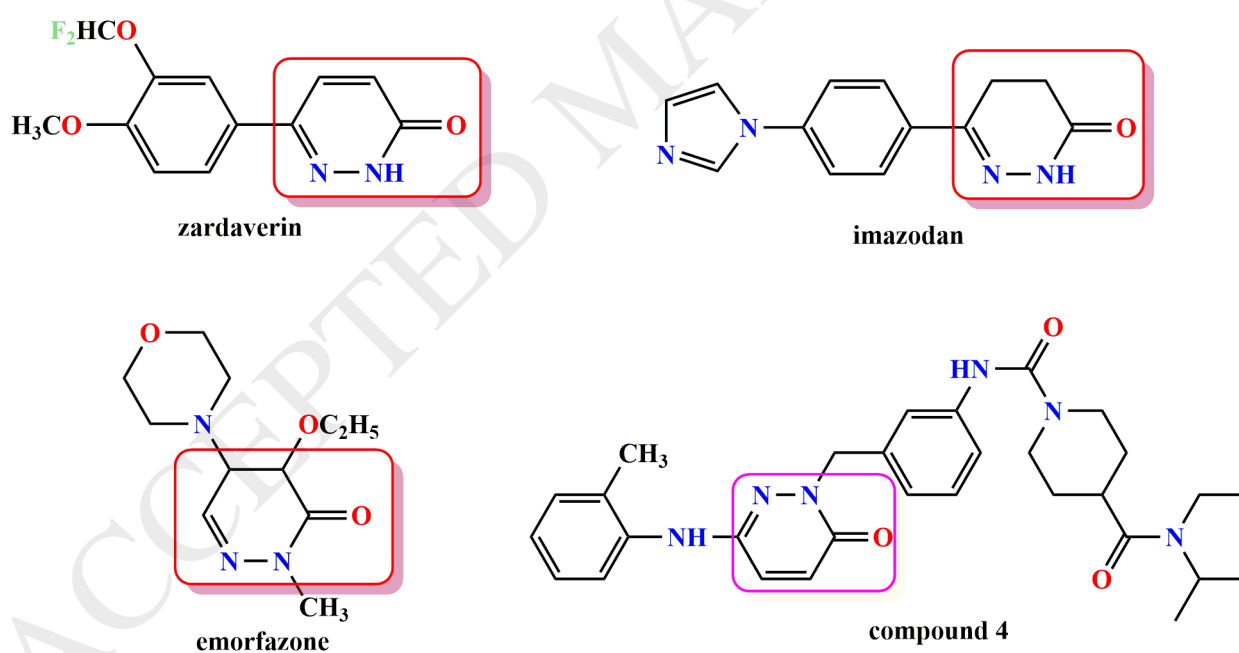
Figure 2. Structure of some FDA-approved AChEI in AD.

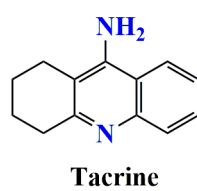**Figure 3.** Structural hypothesis for AChEIs and some designed compounds from the literature [25].
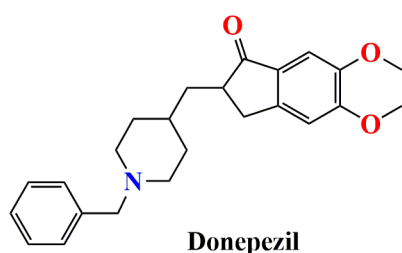
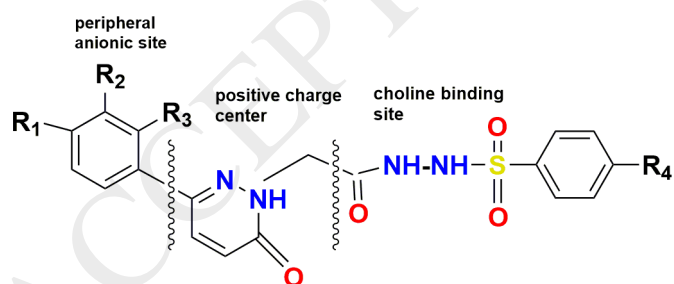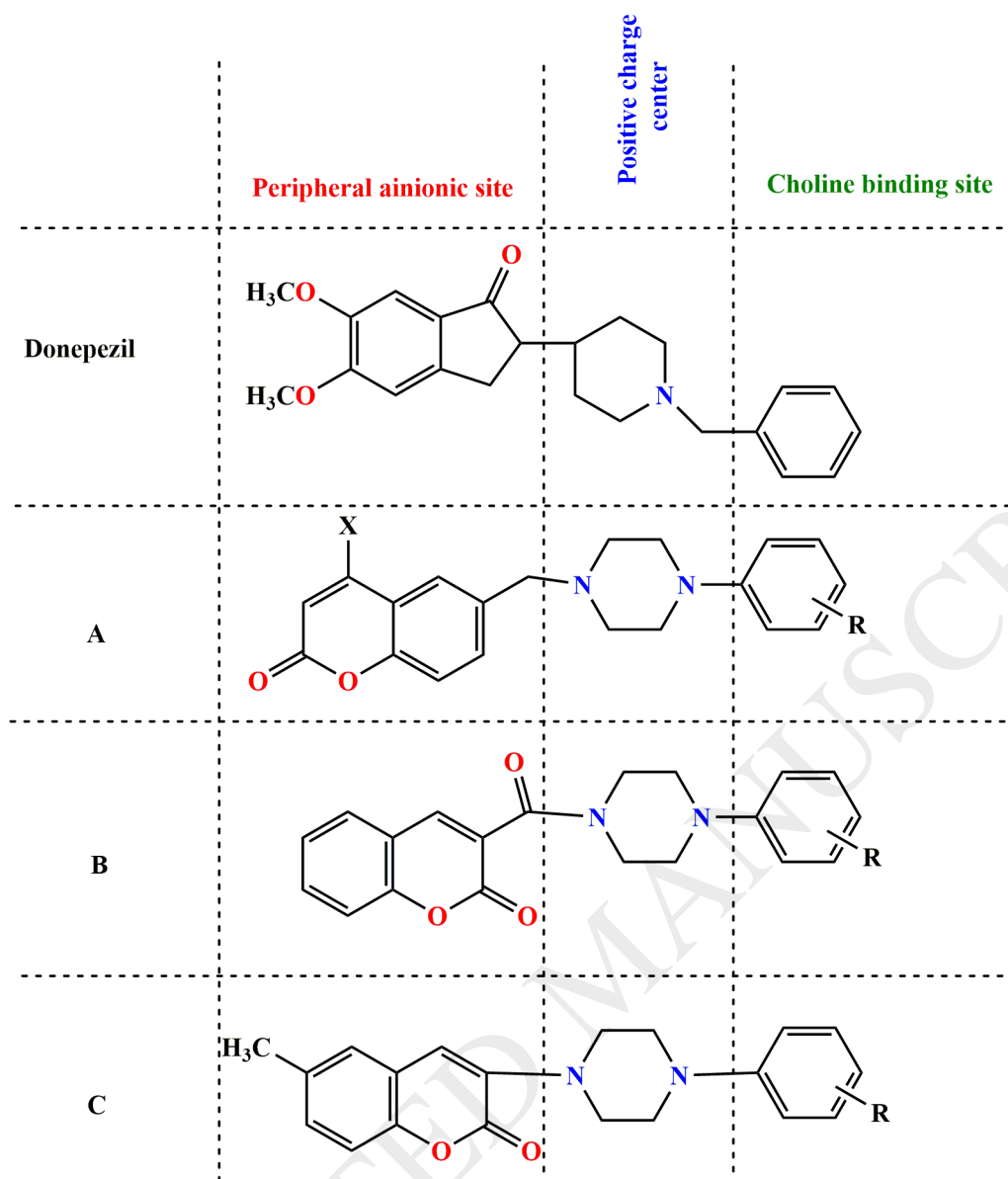**Figure 4.** Structural hypothesis for the title compounds [25].

Figure 5. Binding interaction of RM0 (green), galantmine (gray), **1a** (teal) and **2a** (orange) (A-D, respectively) in EeAChE active gorge. Ligands and water molecules are showed as color sticks, the active gorge residues in sticks and the protein backbone in tubes.

Figure 6. Binding interaction of 3F9 (green), galantmine (gray), **2a** (orange) and **2c** (magenta) (A-D, respectively) in ECBhE active gorge. Ligands and water molecules are showed as color sticks, the active gorge residues in sticks and the protein backbone in tubes.
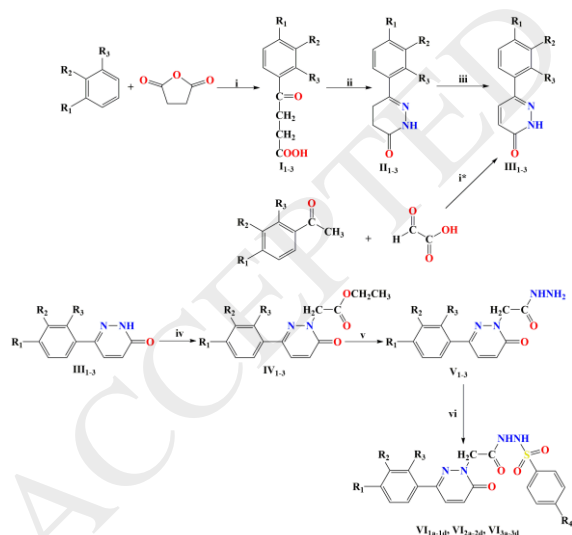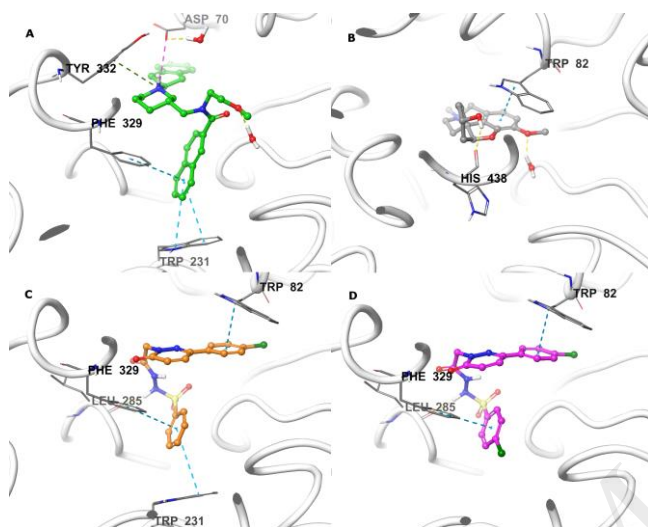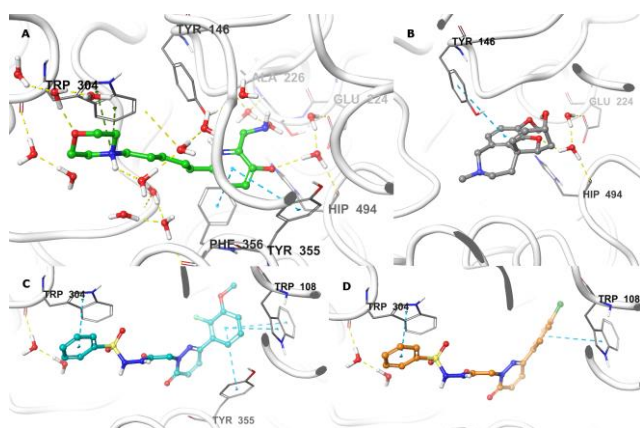
Scheme 1. Synthesis of the **VI$_{1a\text{-}1d}$**, **VI$_{2a\text{-}2d}$**, **VI$_{3a\text{-}3d}$**.

zardaverin

imazodan

emorfazone

compound 4

Donepezil

Tacrine

Ensaculin

Rivastigmine
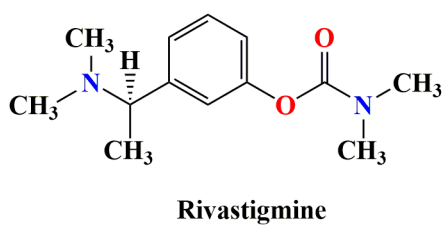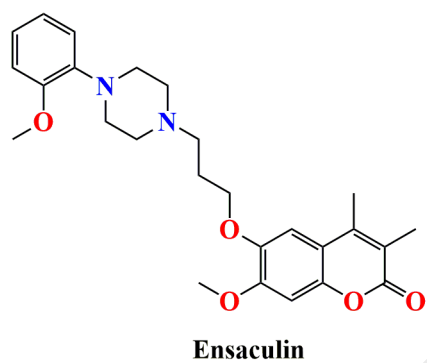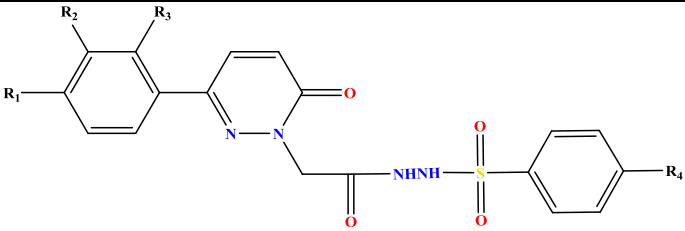
(i) AlCl₃, CS₂ ; (ii) H₂NNH₂, EtOH, reflux (6h); (iii) Br₂, CH₃COOH, reflux (overnight); (i*)
reflux in oil bath (6h), NH₄OH (25%), H₂NNH₂; (i) BrCH₂COOCH₂CH₃, K₂CO₃, aceton, reflux
(overnight); (v) H₂NNH₂.H₂O, MeOH, rt; (vi) ArSO₂Cl, pyridine, 0 °C
R₁: H, Cl, Br; R₂: H, OCH₃; R₃: F, H; R₄: H, Cl, F, CF₃

Table Captions

Table 1. Molecular structures, yields and melting points of **VI$_{1a\text{-}1d}$, VI$_{2a\text{-}2d}$, VI$_{3a\text{-}3d}$**

Table 2. AChE and BChE inhibition percentages of the title compounds with ± standard error mean (SEM)

Table 3. Docking scores

Table 1. Molecular structures, yields and melting points of **VI$_{1a-1d}$, VI$_{2a-2d}$, VI$_{3a-3d}$**

Compound	R$_1$	R$_2$	R$_3$	R$_4$	Yield (%)	MP (ºC)
VI$_{1a}$	-H	-OCH$_3$	-F	-H	59	208
VI$_{1b}$	-H	-OCH$_3$	-F	-F	94	233
VI$_{1c}$	-H	-OCH$_3$	-F	-Cl	89	228
VI$_{1d}$	-H	-OCH$_3$	-F	-CF$_3$	87	240
VI$_{2a}$	-Cl	-H	-H	-H	86	198
VI$_{2b}$	-Cl	-H	-H	-F	79	212
VI$_{2c}$	-Cl	-H	-H	-Cl	86	244
VI$_{2d}$	-Cl	-H	-H	-CF$_3$	82	229
VI$_{3a}$	-Br	-H	-H	-H	78	215
VI$_{3b}$	-Br	-H	-H	-F	73	225
VI$_{3c}$	-Br	-H	-H	-Cl	87	254
VI$_{3d}$	-Br	-H	-H	-CF$_3$	70	255

Table 2. AChE and BChE inhibition percentages of the title compounds with ± standard error mean (SEM)

Compound	AChE 100 μg/ml	BChE 50 μg/ml	BChE 100 μg/ml
VI$_{1a}$	18.71±2.36	7.40±1.28	25.98±2.79
VI$_{1b}$	8.61±1.72	8.46±2.24	22.87±1.53
VI$_{1c}$	-	13.59±1.84	24.65±2.46
VI$_{1d}$	5.11±1.81	9.68±1.54	13.41±2.42
VI$_{2a}$	25.02±1.86	11.95±1.97	51.70±3.93
VI$_{2b}$	8.17±2.34	8.88±0.36	39.59±1.78
VI$_{2c}$	-	21.10±2.24	51.36±3.32
VI$_{2d}$	4.49±1.99	28.55±3.15	43.08±2.18
VI$_{3a}$	4.47±0.47	18.11±3.33	25.34±3.44
VI$_{3b}$	*	11.88±3.14	*
VI$_{3c}$	9.98±1.52	5.45±0.86	43.16±1.98
VI$_{3d}$	*	23.23±2.40	*
Galantamin HCl	90.75±0.02		80.03±1.17
Donepezil**	IC$_{50}$=6.7 nM		
Rivastigmine**	IC$_{50}$=4.3 nM		
Physostigmine**	IC$_{50}$=0.67 nM		
Tacrine*	IC$_{50}$=77 nM		

* percent inhibition could not be determined due to precipitation during the assay

- did not show inhibitory activity

** Reference: Methods and Findings in Experimental and Clinical Pharmacology 22(8):609-13. DOI: 10.1358/mf.2000.22.8.701373. (50 μM)

Table 3. Docking scores

Compound	EeAChE	ECBChE
VI$_{1a}$	-6.44	-6.61
VI$_{1b}$	-6.16	-6.34
VI$_{1c}$	-6.43	-5.51
VI$_{1d}$	-6.32	-5.55
VI$_{2a}$	-6.68	-7.12
VI$_{2b}$	-7.09	-7.41
VI$_{2c}$	-7.14	-7.48
VI$_{2d}$	-6.47	-7.39
VI$_{3a}$	-5.36	-7.13
VI$_{3b}$	-6.71	-6.86
VI$_{3c}$	-5.44	-7.36
VI$_{3d}$	-5.92	-5.04
Galantamine	-6.62	-6.91